Nearly Perfect 3D Structures Obtained by Assembly of Printed Parts of Polyamide Ionene Self-Healing Elastomer

Kathryn O'Harra[1], Naroa Sadaba[2], Mikel Irigoyen[2], Fernando Ruipérez[2], R. Aguirresarobe[2], Haritz Sardon[2], Jason Bara[1*]

*corresponding author: jbara@eng.ua.edu

[1] University of Alabama, Department of Chemical & Biological Engineering, Tuscaloosa, AL 35487-0203

[2] POLYMAT, University of the Basque Country UPV/EHU, Joxe Mari Korta Center, Avda. Tolosa 7, 20018 Donostia-San Sebastian, Spain

KEYWORDS: 3D-Printing, Polymers, Shape Memory, Self-Healing, Ionenes

ABSTRACT: Herein we demonstrate 3D printing of an elastomeric imidazolium polyamide-ionene which exhibits intrinsic shape-memory (SM) and self-healing (SH) character, reporting optimized printing conditions and rheological properties. This study shows the suitability of this material for 3D-printing via fused deposition modeling. The 3D-printed objects retain elasticity and shape memory when external force is applied, and the elastomeric character is quantified via mechanical testing. This work highlights the benefits of SH behavior as a design feature combatting inherent material weaknesses or insufficient adhesion at seams and layer junctions. DFT calculations confirmed the importance of ionic interactions and H-bonding in the healing process.

Introduction

3D-printing has garnered significant attention by researchers and industry due to benefits including faster production, customizability of design and material, minimized waste, high precision, energy efficiency and cost-effectiveness. The utility of 3D-printing technology has been demonstrated in diverse applications within biological (i.e. biotechnology, drug delivery, hydrogels) and chemical (i.e. separations, catalysis) industries. While additive manufacturing technologies have advanced and expanded to include processing of metals, biomaterials, ceramics, concrete, and various composites, polymers dominate as the foundational feedstock for 3D-printing due to the tunability of physical properties, functional flexibility, reactivity suitable for heat or UV-assisted curing, and amenability to form composites.[1, 2]

Fused deposition modeling (FDM) is one of the most common 3D-printing processes, which relies on material heating and extrusion via layer-by-layer deposition, rather than photochemical or laser-induced fusion. It is known that FDM methods impart certain disadvantages, including warping, weakness caused by stress at seams, and decreased bonding strength between adhered layers. These mechanical issues can be combatted through the use of functional materials which have a higher affinity for fusion and layer adhesion. Thus, additive manufacturing research has gravitated toward the use of stimuli-responsive, smart materials, coined as "4D-printing", since 3D printed products consequently exhibit autonomous behavior as a function of time related to the nature of the stimuli.[3-5] For instance, polymers possessing shape-memory (SM) and self-healing (SH) character present a potential solution to the aforementioned mechanical weaknesses, as retention of complex designs is imperative and directionally induced defects or weaknesses resulting from layer-by-layer deposition-based printing techniques are ameliorated by this material fusion response.

These complex SM and SH phenomena, driven by particular chemical and structural features, have been observed and studied in polymeric materials and composites for decades, and are attributed to dynamic bonding or complex intermolecular interactions (i.e. H-bonding, ionic interactions) [6-9]. Polyamides, polyureas, and polyurethanes have exhibited SM and SH features resulting from the regular H-bonding forcing coordination and alignment between chains.[10-14] Polyelectrolytes, ionomers, and ionenes have also been designed to harness these features, due to the strength of ionic interactions coordinating chains.[15-20]

While SM polymers are more common than SH polymers, very few examples of 3D-printing SH polymers, composites, or elastomers have been reported. Works from Long's group have discussed the design of ionic and elastomeric polymers for 3D printing[21-23]. Several groups have investigated 3D-printing of SH polymers using stereolithography (SLA), digital light processing (DLP), or

direct in write (DIW) techniques. However, these examples are all reliant upon crosslinking or dynamic bonding interactions (i.e. Diels-Alder, disulfide chemistries) [2-4][25-26][27-28][29-30]. Additionally, most of these systems which possess SH characteristics involve complex, multicomponent polymeric composites rather than an intrinsically self-healing homogenous polymeric material suitable for extrusion based printing [31-34].

Contributing to limited homogenous SH materials in literature suitable for 4D-printing, O'Harra and Bara recently introduced a series of imidazolium polyamide (PA) ionenes which exhibited excellent, rapid SM and SH behavior at room temperature (hastened at elevated temperatures), resulting from a balance of combined intermolecular forces or chain alignment (Scheme S1)[9, 11, 35]. Additive manufacture of ionic polymeric materials has undoubtably been of interest, due to the potential applicability of composites as soft actuators or in batteries and electronics[36-41]. Ionenes, polymers which incorporate ionic moieties directly within the backbone rather than pendant to the main chain, allow for a great degree of tunability with respect to charge spacing and tolerance to other functionality[42]. Moreover, anion metathesis to the Tf_2N^- form yields a robust, hydrophobic elastomer with intrinsic SH and SM behaviors[9, 11, 35, 43]. This SH behavior was observed through the healing of cuts or punctures. The SM quality, or a return to some initial shape when an external stimulus is applied and then removed (i.e. torsion, folding, molding, tension, compression, imprint), was also observed through manipulation of these bulk PA ionenes. The alternating ionic moieties and H-bonding sites within the terephthamide segments contribute to the distinct thermophysical properties observed in this set of PA ionenes.

Here, we report the first demonstration of 3D-printing of a neat, homogenous ionic elastomer using deposition techniques. These methods allow for the efficient processing of this thermally stable PA-ionene, which retains SH and SM features post-printing. It should be highlighted that the synthesis of these homogenous, functional ionenes is straightforward and scalable, and requires inexpensive, commercially available reagents. The simplistic preparation of this functional ionene via conventional yet tailorable synthetic methods reveals the potential and tunability of ionene derivatives as candidates for 4D printing, without the excessive cost or complexity associated with composites possessing comparable SH and SM properties for high-impact applications. The rheological behavior is studied to guide development and optimization of additive manufacturing conditions, as the intricacies of structured or aligned domains and contributions of intermolecular interactions necessitate defined, controlled processing. Another benefit of this feedstock is the potential for environmentally-friendly fabrication, as this ionene and similar polyurea ionenes were successfully synthesized from PET wastes, demonstrated in our recent work.[9] We took advantage of the outstanding SH ability of this PA ionene to assemble 3D printed 2D parts, subsequently constructed into neat 3D complex geometries.

It is imperative before printing any polymeric material to collect information about the thermal transitions and flow behavior of the material. These experiments impart guidance regarding printing temperature together with the rheological analysis in understanding material flow and optimization of printing speed and pressure. To do so, the material properties of the [TC API pX][Tf_2N] ionene were characterized. Mechanical tests were performed following printing, to determine the retention of elastomeric behavior and alignment effects. Tensile properties were tested to check the ductility of the material after printing and to better understand the influence of printing orientation. The resultant process and optimization of printing procedures is discussed. Demonstrations of printing and products are included. The retention of SH behavior is shown by the union of different 2D-printed parts (with interlocking "teeth") to build a dodecahedron which could hold the assembled 3D shape. This confirms that the material does not lose the SH property after printing, and autonomously fuses the seams and gaps between extruded lines and layers.

The PA-ionene used in this work, denoted [TC API pX][Tf_2N], was introduced and synthesized in our previous works [11, 35]. This involved the condensation of terephthaloyl chloride (TC) and 1-(3-aminopropyl)imidazole (API) to form an amide-containing bis(imidazole), which was subsequently polymerized with para-dichloroxylene (pX) via the Menshutkin reaction, followed by anion metathesis to the bistriflimide form (Tf_2N) (see Scheme S1).

An *Envisiontec* 3D Bioplotter and an *Allevi 3* 3D Bioprinter were utilized with a high-temperature extrusion head. Rheological studies were performed utilizing ARG2 TA Instruments rheometer with a parallel plate fixture 25 mm in diameter. Thermal characterizations were carried out utilizing a Q200 DSC (TA Instruments) at a rate of 5 or 10 °C/min under a nitrogen atmosphere of 50 mL/min, DSC 2920 and thermogravimetric analysis (TA Instruments) was performed under oxygen atmosphere of 20 ml/min. Tensile tests were performed using an Instron 5565 testing machine with a 500 N maximum loading and a crosshead displacement rate of 5 mm min^{-1}. The mechanical properties of the specimens were measured at 21 ± 2 °C and 50 ± 5 % relative humidity (RH) following ASTM D 638. The mechanical properties reported for each material correspond to average values of five experiments.

Structural and functional characterizations (NMR, IR, MS) for this ionene were reported previously[35, 44]. To demonstrate that high-molecular weight polymer suitable for 3D printing was produced, MALDI-TOF MS analysis was used to quantify the number average molecular weight (M_N) of 81 kDa ($X_N \sim 78$ repeat units). The thermal transitions and behaviors were studied using Differential Scanning Calorimetry (DSC), and thermogravimetric analysis (TGA). This PA-ionene exhibits two glass transition temperatures (Figures S2-4). While uncommon, two glass transitions have been observed in some polyamide, polyureas, and ionic polymers[45-47]. The $T_{g,1}$ endotherm is broad and may be due to initial relaxation of structured or aligned domains where intermolecular forces have imparted self-assembly. These ionenes are complex and are organized by the combination of H-bonding, ionic, and stacking (π-π, π-cation) interactions. Alternatively, it may be indicative of anion mobility since the Tf_2N^- anion is large and constitutes a significant mass/volume fraction

of the polymer matrix, contributing more weight given the ratio of the cationic backbone (RU = 484.603 amu) the paired anions (2 Tf_2N^- per RU, 560.272 amu). The primary $T_{g,2}$ endotherm occurs at 55 °C.

TGA demonstrated the thermal stability of this ionene, with a high decomposition onset temperature ($T_{d,onset}$) of 370 °C (Figure S5). Despite drying of the sample at 100 °C in a vacuum oven, some mass loss was a result trapped water or NMP solvent within the ionene. Additional support for the thermal stability was studied by monitoring mass loss as a function of time, showing high mass retention at elevated temperatures, as > 92.5% of mass remained when the ionene was held for 300 minutes at temperatures ranging from 90 - 120 °C (Figure S6).

In addition to the thermal properties, the rheological properties of the material must be defined prior to the printing process. Several rheological experiments were performed in order to investigate the material flow in the printing nozzle (Figure 1). Shear thinning behavior was observed for this PA-ionene, as evidenced by the log-log plot of viscosity versus shear stress at 90 °C and 110 °C Figure 1D). It should be mentioned that the low viscosity values at 110 °C enable the material printing in our experimental setup [48]. In addition, we studied the material consolidation by Small Amplitude Oscillatory Shear (SAOS) experiments at different temperatures (Figures 1A-C). To do so, we selected a frequency of 1 Hz, as it can be considered the reciprocal of the typical adhesion time in 3D printed processes[49]. As shown, the polymer exhibits more viscous then elastic behavior (G' over G'') at high temperatures (i.e. 110 °C). However, as the temperature decreases, the material behavior changes to a more predominant elastic behavior (G' over G''). The intersection of G' and G" falls at 70 °C, above which the molecular dynamics promote polymer interdiffusion amongst consecutive layers [50]. The temperature was 90 °C for Figures 1A-B; the strain amplitude of Figures 1B-C was 1 Hz and these graphs were made in oscillatory mode (Strain: 1x10-4 to 10), and lastly Figure 1D was prepared in continuous mode (flow procedure, shear stress from 100 to 0.1) with a strain percent of 1%.

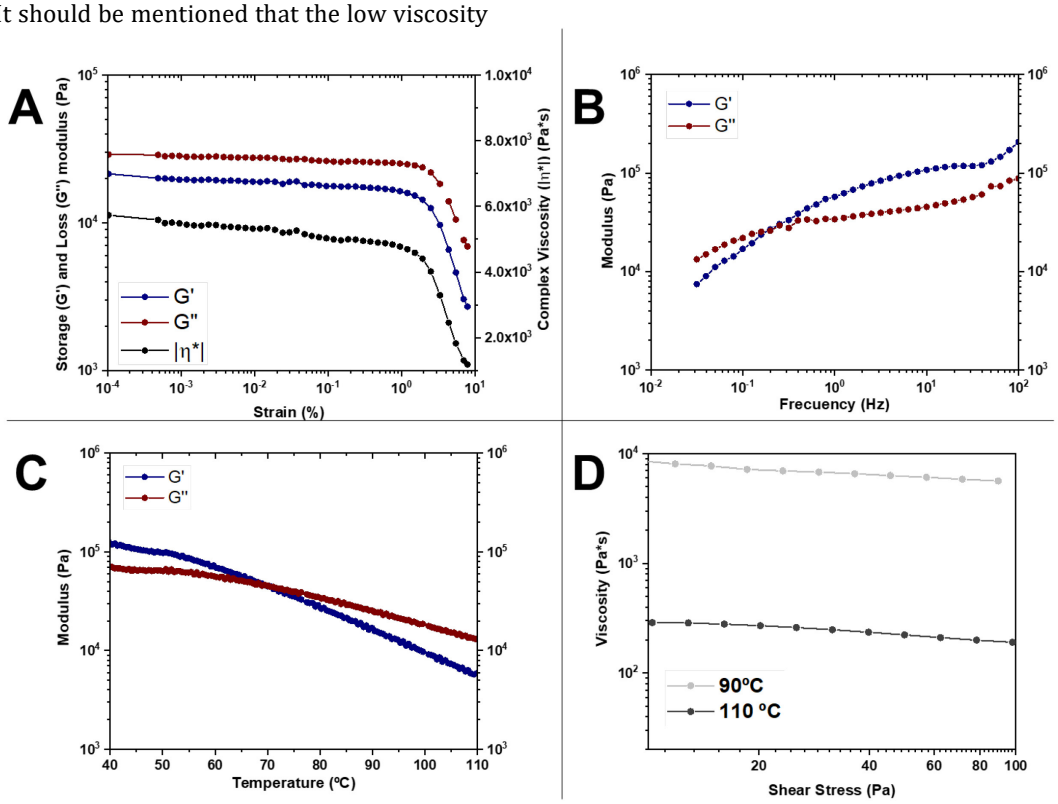

After evaluating the rheological properties, tensile testing of [TC API pX][Tf_2N] was performed utilizing an ASTM standard "dog bone" which was 3D printed, as shown in Figure 2B-C. The goal was to determine the retention of elastomeric behavior and directional chain alignment effects from extruding the material. In order to print the material, an Envisiontec 3D Bioplotter was utilized. This allowed for precise control of temperature and pressure driving extrusion and material flow (Figure 2A). Tensile properties were tested to check the ductility of the material after printing. The printing orientation was alternated (0° and 90°) for the "dog bone", which can be seen in Figures 2B-D. Aided by the fusion of the material layers, the segments perpendicular to the stress direction held up to an elongation of 445%, thus the elastic character was retained. In comparison to the neat ionene, the printed bar was amenable to greater elongation but exhibited a lower modulus[11]. Calculations yielded a Young's Modulus of 1.98 MPa and tensile toughness of 1851 J/m^3 (Table S1). To probe the effects of

printing orientation on SH, bars with unilateral printing orientations (0° or 90°) were tested to better understand the effects of alignment and interlayer adhesion. These samples were investigated using SEM and tested as printed or with a midpoint full cut (perpendicular to the direction of stress), which were allowed to heal for 72 h (Figure 3D/G, 4C, S9). Printing solely at a 0° orientation (i.e. perpendicular to the direction of stress), an elongation at break of 400% could still be obtained. This only decreased to 375% for the sample which possessed an inherently weaker seam due to the cut which was parallel to the infill orientation and allowed to self-heal. Printing solely at a 90° orientation (i.e. parallel to the direction of stress), an increased elongation at break of 600% could be achieved, plausibly due to enhanced elastic behavior contributed by the aligned infill. A decrease to a 400% elongation at break was observed when the sample had been cut at the midpoint and allowed to self-heal at the seam for 24 h, however, the break occurred near the clamped edge rather than at the defect/cut and healed midpoint.

Rheological and thermal characterizations aided in optimizing flow and printing speed. These printing parameters are summarized in Table S2.

Additional qualitative support for the SH and SM behavior of this ionene when subjected to shape manipulation, puncture, compressive, tensile, or torsional stresses is included through several demonstrations (Video S1). Figure 3 highlights the SH performance of the ionene, with SEM images captured following 24 h at RT, to represent the interface characteristics of an extrusion-based, 3D printed material. The fusion and interlayer adhesion of the PA ionene was observed through the erasing of seams in varied geometries (Figure 3A) through sheet and fiber layering (Figure 3B-C), coiling (Figure 3E), and precise slicing of the ionene with a razor blade (Figure 3F). Comparison of cleanly cut seams and the adhesion of interlayer gaps is shown in Figures 3D/G, 4C, S9. PLM images were also obtained, exhibiting the healing of seams in a cut ionene film (Figure S7) and the effects of chain alignment which occur upon extrusion or tensile stresses resulting in induced opacity and unidirectional ordering (Figure S8).

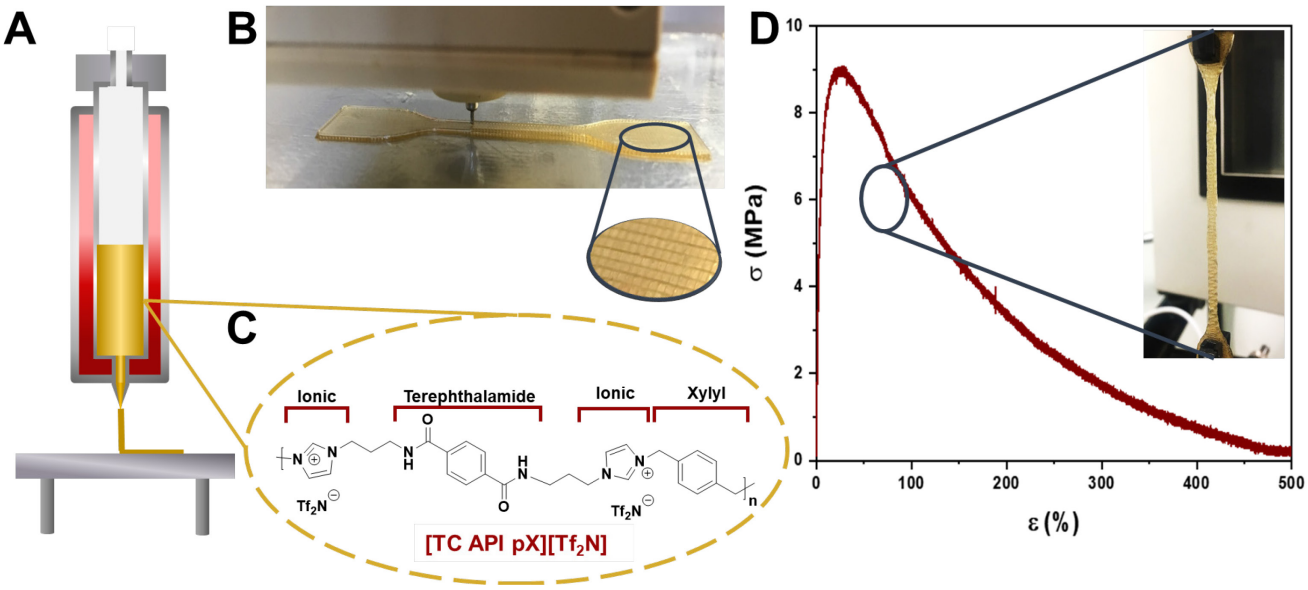

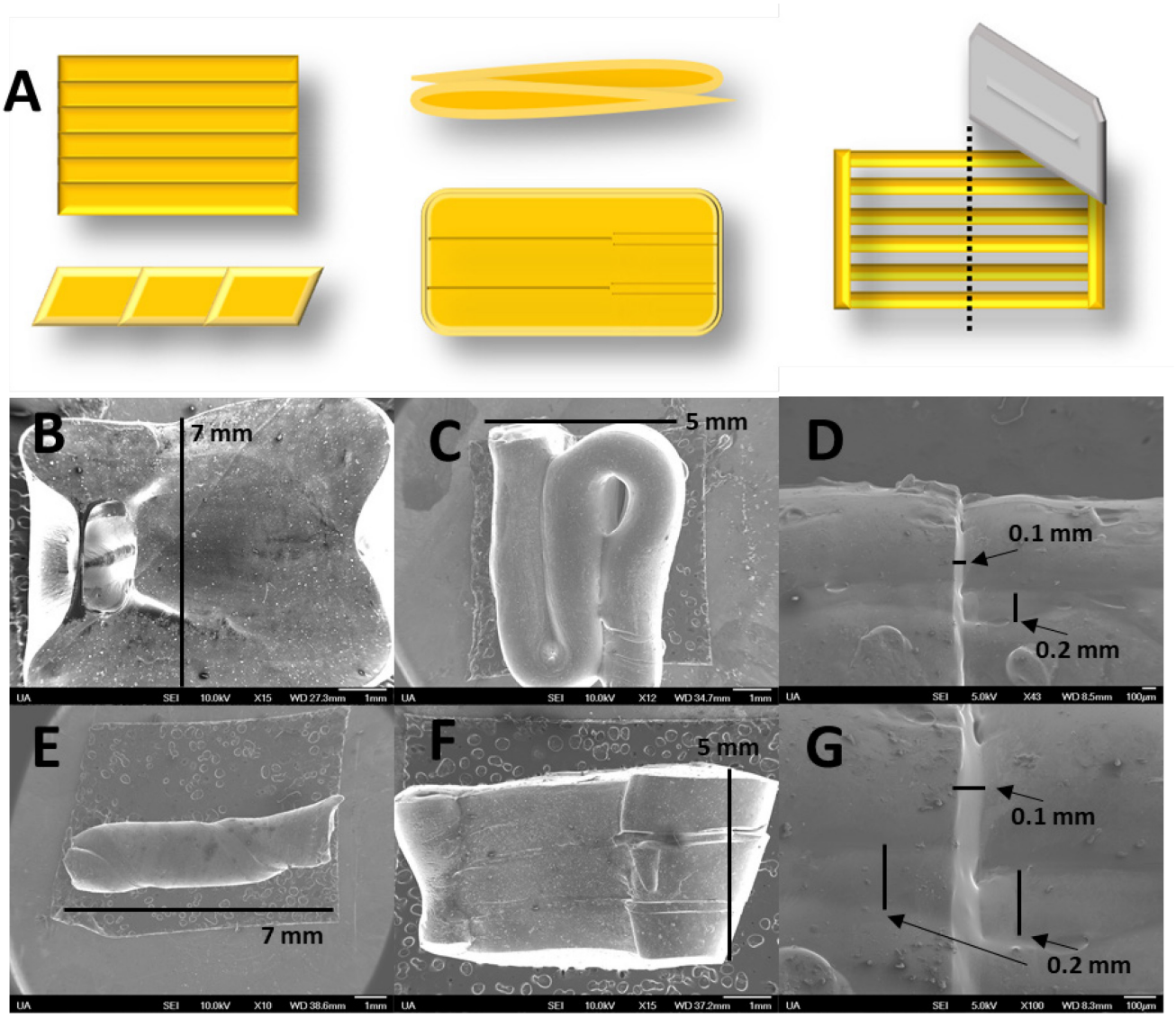

Figure 3. [A] Representation of SH demonstration geometries; [B] cross-section via SEM of stacked, 6-layer cross-section via SEM of fused ionene; [C] cross-section via SEM of fused fiber; [D] cut perpendicular seam at edge of a self-healed 3D-printed bar; [E] top view via SEM of fused twist; [F] top view via SEM of sliced ionene; [G] cut seam and healed interlayer gaps within a 3D-printed bar.

In addition to the alternating "dog bone" and the unilaterally printed 3D bars for tensile testing, one particularly influential area to employ SH materials is the manufacturing of 2D parts which can later be assembled into their final 3D geometry. This could make shipping volumetrically efficient, reducing environmental impact (Figure 4). To emphasize the SM and SH behaviors, several pentagonal objects were printed with notches around the periphery. These were subsequently assembled into halves of a dodecahedron. After 24 h, the PA-ionene had fused and healed, and the seams located at the interlocking notches disappeared. The full dodecahedron geometry was retained upon assembly, while the lines between the "teeth" forming the junctions became smoother. Figure 4 depicts these printed building blocks and the resultant structures.

In order to gain insight into the unique SH behavior of PA-ionenes, we have performed molecular dynamics (MD) simulations to study the nature of the H-bonding in this material. The structuring and interactions between ionene chains are influenced by the combination of intermolecular interactions, which dictate the SM and SH features. Table 1 summarizesthe numerical analysis of the H-bonding data collected.

Table 1. Number of hydrogen bonds (nHB) between domains of the polymeric chain and percentage of interactions in brackets.

Interacting Segments		nHB (%)
Tf_2N	Imidazolium	1386924 (40.96)
	Terephthalamide	1167687 (34.48)
	Xylene	196508 (5.80)
Terephthalamide	Imidazolium	261207 (7.71)
	Xylene	30643 (0.90)
Imidazolium	Xylene	7449 (0.22)

Three domains are defined in the polymeric chain to analyze the non-covalent interactions in the material, together with the Tf_2N anion, namely, imidazolium, terephthalamide and xylene (see Figure 2C).

The highest number of hydrogen bonds is established by the anion (Tf_2N), as expected considering that it is a mobile molecule that can interact with the surroundings. Thus, the H-bonding of Tf_2N with the cationic part of the chain (imidazolium) accounts for 40.96% of total interactions, since in each repeating unit there are two cation-anion pairs and the ionic interaction maintains the proximity of these units, favoring the formation of hydrogen bonds. The second largest value corresponds to the interaction between Tf_2N and the terephthalamide domain of the chain (34.48%), due to the presence of N-H groups, prone to form hydrogen bonds. The hydrogen bonds established with the xylene domain amount only 5.80% of the total, since there are no moieties susceptible to interact effectively via H-bonding.

The lowest values correspond to the interactions among the three domains of the chain (terephthalamide, imidazolium and xylene), which suggest that the intermolecular interactions take place by means of the anions with the surrounding chains.

In order to further analyze the non-covalent interactions in the material, density functional theory (DFT) calculations have also been performed in a small model consisting of two repeating units. The interaction energy of these two chains is -120.23 $kJ \cdot mol^{-1}$, a high value comprised of electrostatic, hydrogen bonding, and π-π stacking interactions in cooperation. Thus, inspecting the nature of the H-bonding in the system, Tf_2N may establish hydrogen bonds mainly with the sulfonyl group, and rather short S=O···H-N distances are observed (between 1.930 and 1.980 Å). Furthermore, H-bonding is also observed between trifluoromethyl groups (CF_3) and amide (N-H) moieties of terephthalamide. This suggests rather strong H-bonding interactions. Finally, weak π-π stacking interactions are expected due to the intricate network with a high degree of entanglement, as a consequence of the H-bonds. Thus, the probability to find benzyl rings close enough and in a proper conformation to interact is small. In summary, the SM and SH features in these systems may be ascribed mainly to the H-bonding interactions of Tf_2N anions with the surrounding chains, reinforced by the electrostatic interactions with the imidazolium moiety. This computational work is highlighted in Figure 5, and specific computational details are included as supporting information.

Conclusions

We have demonstrated processing of a neat, homogenous PA-ionene via deposition-based 3D-printing and shown that SM and SH behavior is retained. Computational analysis was reported to illustrate the relative contributions of ionic, H-bonding, and stacking interactions which influence these behaviors. The thermal and rheological properties were probed in order to optimize printing conditions, as well as gain a better understanding of material flow and stimuli response. This work highlights the importance of designing smart, high-performance polymers which possess SH and SM behavior simply though structural features without the requirement of fillers or multiple components. Focusing on dynamic behaviors in the design of polymers for additive manufacturing may pave the way for combatting inherent weaknesses in layer-by-layer 3D-printing, without sacrifice of homogeneity and desirable thermophysical properties.

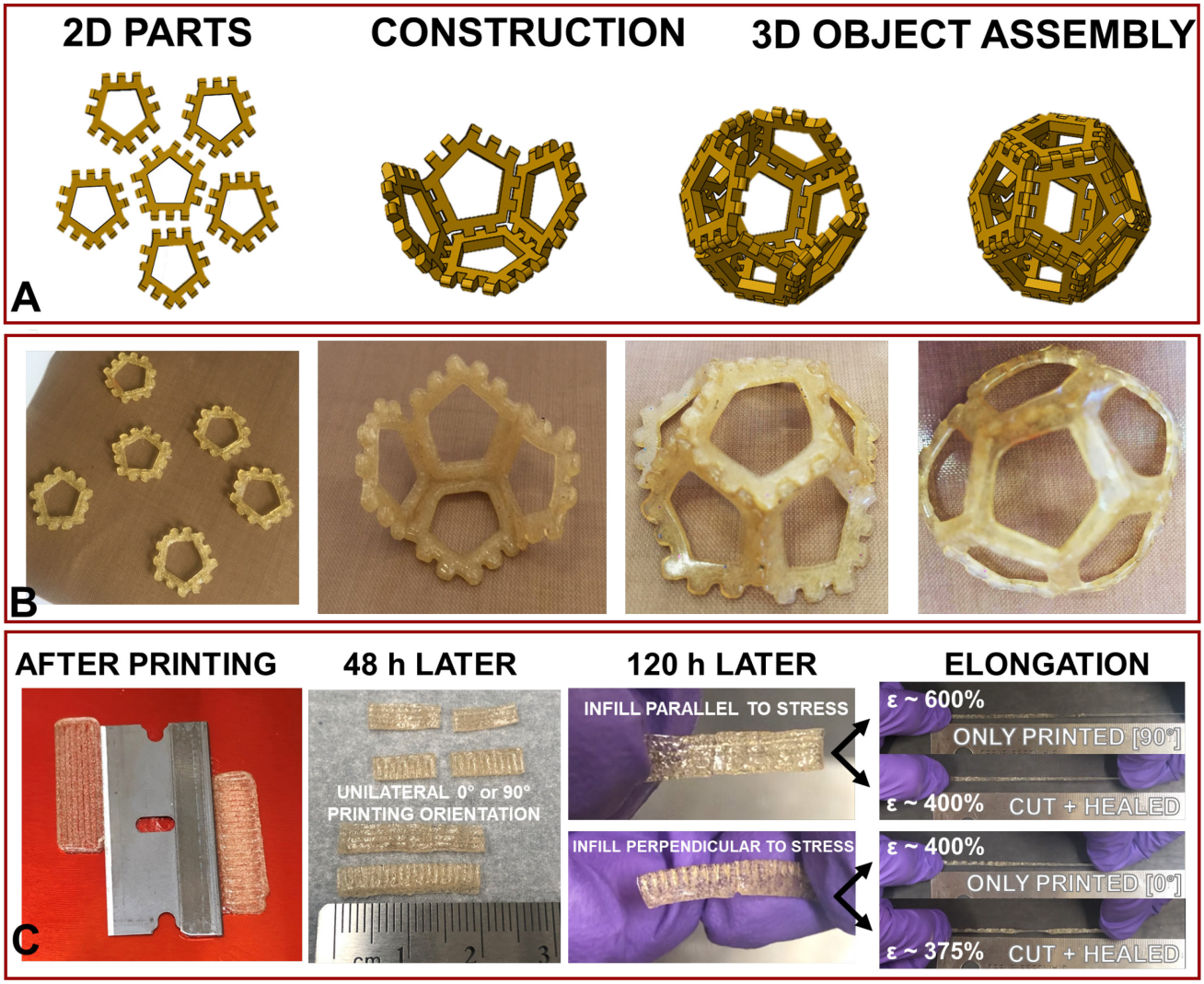

Figure 4. CAD depictions [A] and 3D-printed pentagon parts [B] with interlocking teeth, constructed into a dodecahedron. The seams at each joint was shown to heal within 24 h, and the combination of each half into a 3D-geometry demonstrated self-healing and shape retention for several days. [C] Printed bars with purely 0° or 90° infill orientations over time, highlighting retention of resolution and effects on tensile properties. As a result of altered adhesion at interlayer seams and healed interfaces after cutting perpendicular to the direction of stress, elongation at break and strength was affected.

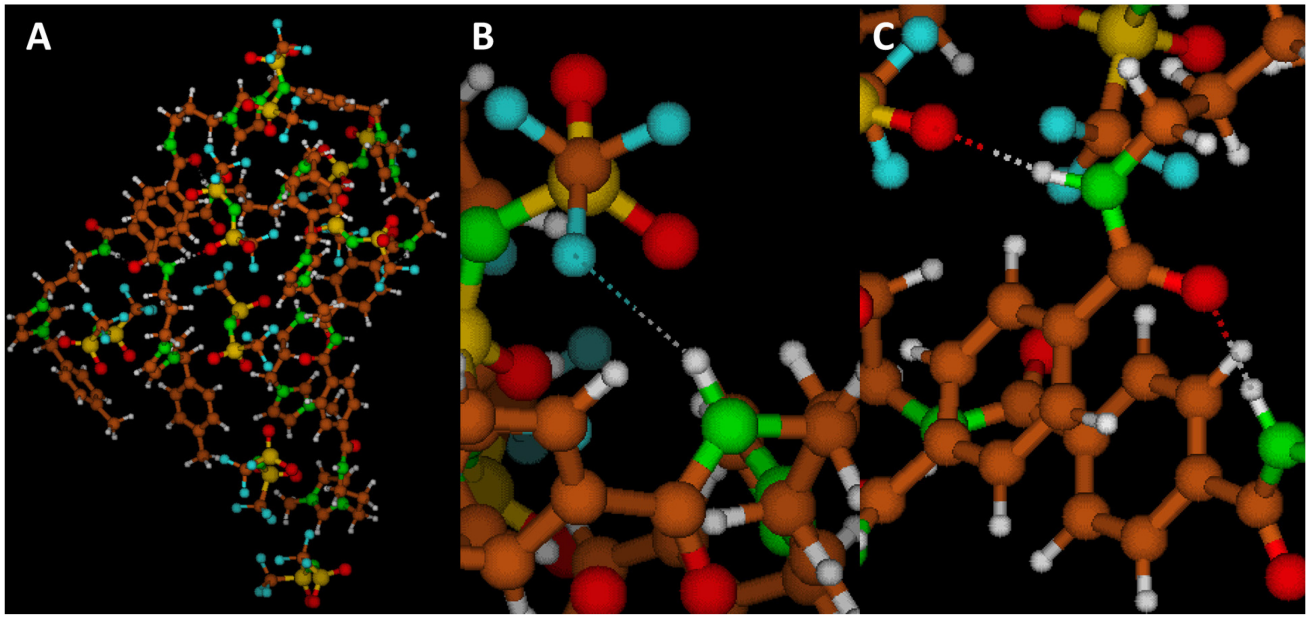

Figure 5. Simulation images highlighting [A] repeat unit conformation, [B] C-F···H-N interactions, and [C] S=O···H-N interactions. Atoms are distinguished by the following coloration scheme: C (orange), H (gray), N (green), O (red), S (yellow), F (teal).

ASSOCIATED CONTENT

Supporting Information. Additional thermal or structural characterization plots and printing condition details are included as Supporting Information. Demonstration videos qualitatively and quantitatively highlighting the SH and SM behaviors (via shape modifications, puncture or cut defects, or from compressive, torsional, and tensile stresses on samples with unilateral printing orientations) have been prepared and included as Supporting Information. This material is available free of charge via the Internet at http://pubs.acs.org."

AUTHOR INFORMATION

Corresponding Author

* Corresponding author: Prof. Jason E. Bara.

Author Contributions

The manuscript was written through experimental and analytical contributions of all authors. Material design, synthetic work, and characterizations were completed by K.E. O'Harra and J. Bara. Rheological studies and additive manufacturing were completed by R. Aguirresarobe, N. Sadaba, H. Sardon, and K. O'Harra. Computational studies were completed by M. Irigoyen and F. Ruipérez. The formation, writing and discussion of data, and review of this manuscript was led by K. O'Harra. All authors have given approval to the final version of the manuscript.

Funding Sources

Support from the National Science Foundation (CBET 1605411) is gratefully acknowledged. The authors thank MINECO for the grant MAT2017-83373-R.

Conflict of Interest

The authors declare no conflicts of interest.

ACKNOWLEDGMENT

The authors thank for technical and human support provided by SGIker (UPV/EHU, ERDF, EU). The authors would like to acknowledge Prof. John Kim (University of Alabama) for allowing the use of the Allevi 3 Bioprinter in his laboratory. J. E. Bara thanks Prof. David Mecerreyes for hosting his visit to San Sebastian and POLYMAT during Sept. – Nov. 2018.

ABBREVIATIONS

PA: polyamide; SM: shape-memory; SH: self-healing; NMR: nuclear magnetic resonance; HRMS: high-resolution mass spectrometry; IR: infrared spectroscopy; MALDI-TOF MS: matrix-assisted laser desorption ionization time-of-flight mass spectrometry; [TC API pX][Tf_2N]: polyamide ionene utilized in this work; X_N: number average degree of polymerization; M_N: number average molecular weight; RU: repeat unit; DFT: density functional theory; MD: molecular dynamics

REFERENCES

1. Wang, X.; Jiang, M.; Zhou, Z.; Gou, J.; Hui, D., 3D printing of polymer matrix composites: A review and prospective. *Composites Part B: Engineering* **2017,** *110*, 442-458.
2. Ngo, T. D.; Kashani, A.; Imbalzano, G.; Nguyen, K. T. Q.; Hui, D., Additive manufacturing (3D printing): A review of materials, methods, applications and challenges. *Composites Part B: Engineering* **2018,** *143*, 172-196.
3. Momeni, F.; M.Mehdi Hassani.N, S.; Liu, X.; Ni, J., A review of 4D printing. *Materials & Design* **2017,** *122*, 42-79.
4. Oliveira, J.; Correia, V.; Castro, H.; Martins, P.; Lanceros-Mendez, S., Polymer-based smart materials by

printing technologies: Improving application and integration. *Additive Manufacturing* **2018,** *21*, 269-283.
5. Lee, A. Y.; An, J.; Chua, C. K., Two-Way 4D Printing: A Review on the Reversibility of 3D-Printed Shape Memory Materials. *Engineering* **2017,** *3* (5), 663-674.
6. Peponi, L.; Navarro-Baena, I.; Kenny, J. M., 7 - Shape memory polymers: properties, synthesis and applications. In *Smart Polymers and their Applications*, Aguilar, M. R.; San Román, J., Eds. Woodhead Publishing: 2014; pp 204-236.
7. Yang, Y.; Urban, M. W., Self-healing polymeric materials. *Chemical Society Reviews* **2013,** *42* (17), 7446-7467.
8. Amaral, A. J. R.; Pasparakis, G., Stimuli responsive self-healing polymers: gels, elastomers and membranes. *Polymer Chemistry* **2017,** *8* (42), 6464-6484.
9. Demarteau, J.; O'Harra, K. E.; Bara, J. E.; Sardon, H., Valorization of plastic wastes for the synthesis of imidazolium based self-supported elastomeric ionenes. *ChemSusChem* **2020**.
10. Faghihnejad, A.; Feldman, K. E.; Yu, J.; Tirrell, M. V.; Israelachvili, J. N.; Hawker, C. J.; Kramer, E. J.; Zeng, H., Adhesion and Surface Interactions of a Self-Healing Polymer with Multiple Hydrogen-Bonding Groups. *Advanced Functional Materials* **2014,** *24* (16), 2322-2333.
11. Kammakakam, I.; O'Harra, K. E.; Dennis, G. P.; Jackson, E. M.; Bara, J. E., Self-healing imidazolium-based ionene-polyamide membranes: an experimental study on physical and gas transport properties. *Polymer International* **2019**.
12. Yang, Y.; Lu, X.; Wang, W., A tough polyurethane elastomer with self-healing ability. *Materials & Design* **2017,** *127*, 30-36.
13. Wang, Z.; Gangarapu, S.; Escorihuela, J.; Fei, G.; Zuilhof, H.; Xia, H., Dynamic covalent urea bonds and their potential for development of self-healing polymer materials. *Journal of Materials Chemistry A* **2019,** *7* (26), 15933-15943.
14. Chen, S.; Mo, F.; Yang, Y.; Stadler, F. J.; Chen, S.; Yang, H.; Ge, Z., Development of zwitterionic polyurethanes with multi-shape memory effects and self-healing properties. *Journal of Materials Chemistry A* **2015,** *3* (6), 2924-2933.
15. Cavicchi, K. A.; Pantoja, M.; Cakmak, M., Shape memory ionomers. *Journal of Polymer Science Part B: Polymer Physics* **2016,** *54* (14), 1389-1396.
16. Fang, X.; Sun, J., One-Step Synthesis of Healable Weak-Polyelectrolyte-Based Hydrogels with High Mechanical Strength, Toughness, and Excellent Self-Recovery. *ACS Macro Letters* **2019**, 500-505.
17. Häring, M.; Grijalvo, S.; Haldar, D.; Saldías, C.; Díaz, D. D., Polymer topology-controlled self-healing properties of polyelectrolyte hydrogels based on DABCO-containing aromatic ionenes. *European Polymer Journal* **2019,** *115*, 221-224.
18. Guan, Y.; Cao, Y.; Peng, Y.; Xu, J.; Chen c, A. S. C., Complex of polyelectrolyte network with surfactant as novel shape memory networks. *Chemical Communications* **2001,** (17), 1694-1695.
19. Jo, Y. H.; Zhou, B.; Jiang, K.; Li, S.; Zuo, C.; Gan, H.; He, D.; Zhou, X.; Xue, Z., Self-healing and shape-memory solid polymer electrolytes with high mechanical strength facilitated by a poly(vinyl alcohol) matrix. *Polymer Chemistry* **2019,** *10* (48), 6561-6569.
20. Wu, W.; Zhou, Y.; Li, J.; Wan, C., Shape memory and self-healing behavior of styrene–butadiene–styrene/ethylene-methacrylic acid copolymer (SBS/EMAA) elastomers containing ionic interactions. *Journal of Applied Polymer Science* **2020,** *137* (19), 48666.
21. Zawaski, C. E.; Wilts, E. M.; Chatham, C. A.; Stevenson, A. T.; Pekkanen, A. M.; Li, C.; Tian, Z.; Whittington, A. R.; Long, T. E.; Williams, C. B., Tuning the material properties of a water-soluble ionic polymer using different counterions for material extrusion additive manufacturing. *Polymer* **2019,** *176*, 283-292.
22. Herzberger, J.; Sirrine, J. M.; Williams, C. B.; Long, T. E., Polymer Design for 3D Printing Elastomers: Recent Advances in Structure, Properties, and Printing. *Progress in Polymer Science* **2019,** *97*.
23. Chen, X.; Zawaski, C. E.; Spiering, G. A.; Liu, B.; Orsino, C. M.; Moore, R. B.; Williams, C. B.; Long, T. E., Quadruple Hydrogen Bonding Supramolecular Elastomers for Melt Extrusion Additive Manufacturing. *ACS Appl Mater Interfaces* **2020**.
24. Yu, K.; Xin, A.; Du, H.; Li, Y.; Wang, Q., Additive manufacturing of self-healing elastomers. *NPG Asia Materials* **2019,** *11* (1).
25. Liu, Z.; Hong, P.; Huang, Z.; Zhang, T.; Xu, R.; Chen, L.; Xiang, H.; Liu, X., Self-healing, reprocessing and 3D printing of transparent and hydrolysis-resistant silicone elastomers. *Chemical Engineering Journal* **2020,** *387*, 124142.
26. Li, X.; Yu, R.; He, Y.; Zhang, Y.; Yang, X.; Zhao, X.; Huang, W., Self-Healing Polyurethane Elastomers Based on a Disulfide Bond by Digital Light Processing 3D Printing. *ACS Macro Letters* **2019,** *8* (11), 1511-1516.
27. Zhou, Q.; Gardea, F.; Sang, Z.; Lee, S.; Pharr, M.; Sukhishvili, S. A., A Tailorable Family of Elastomeric-to-Rigid, 3D Printable, Interbonding Polymer Networks. *Advanced Functional Materials* **2020,** *n/a* (n/a), 2002374.
28. Invernizzi, M.; Turri, S.; Levi, M.; Suriano, R., 4D printed thermally activated self-healing and shape memory polycaprolactone-based polymers. *European Polymer Journal* **2018,** *101*, 169-176.
29. Suriano, R.; Bernasconi, R.; Magagnin, L.; Levi, M., 4D Printing of Smart Stimuli-Responsive Polymers. *Journal of The Electrochemical Society* **2019,** *166* (9), B3274-B3281.
30. Zhang, B.; Zhang, W.; Zhang, Z.; Zhang, Y.-F.; Hingorani, H.; Liu, Z.; Liu, J.; Ge, Q., Self-Healing Four-Dimensional Printing with an Ultraviolet Curable Double-Network Shape Memory Polymer System. *ACS Applied Materials & Interfaces* **2019,** *11* (10), 10328-10336.
31. Kuang, X.; Chen, K.; Dunn, C. K.; Wu, J.; Li, V. C. F.; Qi, H. J., 3D Printing of Highly Stretchable, Shape-Memory, and Self-Healing Elastomer toward Novel 4D Printing. *ACS Applied Materials & Interfaces* **2018,** *10* (8), 7381-7388.

32. Kee, S.; Haque, M. A.; Corzo, D.; Alshareef, H. N.; Baran, D., Self-Healing and Stretchable 3D-Printed Organic Thermoelectrics. *Advanced Functional Materials* **2019,** *29* (51).
33. Wu, Q.; Zou, S.; Gosselin, F. P.; Therriault, D.; Heuzey, M.-C., 3D printing of a self-healing nanocomposite for stretchable sensors. *Journal of Materials Chemistry C* **2018,** *6* (45), 12180-12186.
34. Zhang, Y.; Yin, X.-Y.; Zheng, M.; Moorlag, C.; Yang, J.; Wang, Z. L., 3D printing of thermoreversible polyurethanes with targeted shape memory and precise in situ self-healing properties. *Journal of Materials Chemistry A* **2019,** *7* (12), 6972-6984.
35. Bara, J. E.; O'Harra, K. E.; Durbin, M. M.; Dennis, G. P.; Jackson, E. M.; Thomas, B.; Odutola, J. A., Synthesis and Characterization of Ionene-Polyamide Materials as Candidates for New Gas Separation Membranes. *MRS Adv* **2018,** *3* (52), 3091-3102.
36. Nulwala, H.; Mirjafari, A.; Zhou, X., Ionic liquids and poly(ionic liquid)s for 3D printing – A focused mini-review. *European Polymer Journal* **2018,** *108*, 390-398.
37. Ndefru, B. G.; Ringstrand, B. S.; Diouf, S. I. Y.; Seifert, S.; Leal, J. H.; Semelsberger, T. A.; Dreier, T. A.; Firestone, M. A., Multiscale additive manufacturing of polymers using 3D photo-printable self-assembling ionic liquid monomers. *Molecular Systems Design & Engineering* **2019**.
38. Ahmed, K.; Kawakami, M.; Khosla, A.; Furukawa, H., Soft, conductive nanocomposites based on ionic liquids/carbon nanotubes for 3D printing of flexible electronic devices. *Polymer Journal* **2019,** *51* (5), 511-521.
39. Deiner, L. J.; Jenkins, T.; Howell, T.; Rottmayer, M., Aerosol Jet Printed Polymer Composite Electrolytes for Solid-State Li-Ion Batteries. *Advanced Engineering Materials* **2019,** *21* (12), 1900952.
40. Chen, Q.; Xu, R.; He, Z.; Zhao, K.; Pan, L., Printing 3D Gel Polymer Electrolyte in Lithium-Ion Microbattery Using Stereolithography. *Journal of The Electrochemical Society* **2017,** *164* (9), A1852-A1857.
41. Carrico, J. D.; Hermans, T.; Kim, K. J.; Leang, K. K., 3D-Printing and Machine Learning Control of Soft Ionic Polymer-Metal Composite Actuators. *Sci Rep* **2019,** *9* (1), 17482.
42. Bara, J. E.; O'Harra, K. E., Recent Advances in the Design of Ionenes: Toward Convergence with High-Performance Polymers. *Macromolecular Chemistry and Physics* **2019**.
43. Tan, J. P. K.; Tan, J.; Park, N.; Xu, K.; Chan, E. D.; Yang, C.; Piunova, V. A.; Ji, Z.; Lim, A.; Shao, J.; Bai, A.; Bai, X.; Mantione, D.; Sardon, H.; Yang, Y. Y.; Hedrick, J. L., Upcycling Poly(ethylene terephthalate) Refuse to Advanced Therapeutics for the Treatment of Nosocomial and Mycobacterial Infections. *Macromolecules* **2019,** *52* (20), 7878-7885.
44. O'Harra, K. E.; Kammakakam, I.; Devriese, E. M.; Noll, D. M.; Bara, J. E.; Jackson, E. M., Synthesis and Performance of 6FDA-Based Polyimide-Ionenes and Composites with Ionic Liquids as Gas Separation Membranes. *Membranes (Basel)* **2019,** *9* (7).
45. Boyer, R. F., An apparent double glass transition in semicrystalline polymers. *Journal of Macromolecular Science, Part B* **1973,** *8* (3-4), 503-537.
46. Reinecker, M.; Soprunyuk, V.; Fally, M.; Sanchez-Ferrer, A.; Schranz, W., Two glass transitions of polyurea networks: effect of the segmental molecular weight. *Soft Matter* **2014,** *10* (31), 5729-38.
47. Eisenberg, A., Glass Transitions in Ionic Polymers. *Macromolecules* **1971,** *4* (1), 125-128.
48. Calafel, M. I.; Aguirresarobe, R. H.; Sadaba, N.; Boix, M.; Conde, J. I.; Pascual, B.; Santamaria, A., Tuning the viscoelastic features required for 3D printing of PVC-acrylate copolymers obtained by single electron transfer-degenerative chain transfer living radical polymerization (SET-DTLRP). *Express Polymer Letters* **2018,** *12* (9), 824-835.
49. Seppala, J. E.; Migler, K. D., Infrared thermography of welding zones produced by polymer extrusion additive manufacturing. *Additive Manufacturing* **2016,** *12*, 71-76.
50. Seppala, J. E.; Hoon Han, S.; Hillgartner, K. E.; Davis, C. S.; Migler, K. B., Weld formation during material extrusion additive manufacturing. *Soft Matter* **2017,** *13* (38), 6761-6769.

For Table of Contents Graphic Only